Virology 408 (2010) 49–56

Contents lists available at ScienceDirect

Virology

journal homepage: www.elsevier.com/locate/yviro

Deep sequencing analysis of viral short RNAs from an infected Pinot Noir grapevine

Vitantonio Pantaleo [a,*,1], Pasquale Saldarelli [b,*,1], Laura Miozzi [a], Annalisa Giampetruzzi [c], Andreas Gisel [d], Simon Moxon [e], Tamas Dalmay [e], György Bisztray [f], Jozsef Burgyan [a,*]

[a] Istituto di Virologia Vegetale del C.N.R. Strada delle Cacce 73, 10135, Torino, Italy
[b] Istituto di Virologia Vegetale del C.N.R. Unità Organizzativa di Bari via Amendola 165/A, 70126, Bari, Italy
[c] Dipartimento di Protezione delle Piante e Microbiologia Applicata, Università di Bari, 70126, Bari, Italy
[d] Istituto di Tecnologie Biomediche del C.N.R., Sezione di Bari via Amendola 122/O, 70126, Bari, Italy
[e] School of Computing Sciences, University of East Anglia, NR4 7TJ, Norwich, UK
[f] Corvinus University, Budapest, Hungary

ARTICLE INFO

Article history:
Received 23 June 2010
Returned to author for revision 16 July 2010
Accepted 1 September 2010
Available online 26 September 2010

Keywords:
Grapevine
Tymovirus
Short RNAs
Deep sequencing
RNA silencing

ABSTRACT

Virus-derived short interfering RNAs (vsiRNAs) isolated from grapevine *V. vinifera* Pinot Noir clone ENTAV 115 were analyzed by high-throughput sequencing using the Illumina Solexa platform. We identified and characterized vsiRNAs derived from grapevine field plants naturally infected with different viruses belonging to the genera *Foveavirus*, *Maculavirus*, *Marafivirus* and *Nepovirus*. These vsiRNAs were mainly of 21 and 22 nucleotides (nt) in size and were discontinuously distributed throughout *Grapevine rupestris stem-pitting associated virus* (GRSPaV) and *Grapevine fleck virus* (GFkV) genomic RNAs. Among the studied viruses, GRSPaV and GFkV vsiRNAs had a 5′ terminal nucleotide bias, which differed from that described for experimental viral infections in *Arabidopsis thaliana*. VsiRNAs were found to originate from both genomic and antigenomic GRSPaV RNA strands, whereas with the grapevine tymoviruses GFkV and Grapevine Red Globe associated virus (GRGV), the large majority derived from the antigenomic viral strand, a feature never observed in other plant–virus interactions.

Introduction

RNA silencing regulates several biological processes such as developmental timing and patterning, transposon control, DNA methylation and chromatin modification as well as antiviral defence (Csorba et al., 2009).

RNA silencing relies on small RNA (sRNA) molecules 21–24 nucleotides long, called short interfering (si) RNAs and micro-RNAs (miRNAs) (Hamilton et al., 2002; Hamilton and Baulcombe, 1999; Kim, 2005; Plasterk, 2002). RNA silencing pathways are triggered by double-stranded (ds) or self-complementary foldback RNAs that are processed into 21–24 nt siRNA or miRNA duplexes by RNase III-type DICER enzymes (Bartel, 2004; Baulcombe, 2004; Bernstein et al., 2001). These miRNAs and siRNAs activate a multiprotein effector complex, the RNA-Induced Silencing Complex (RISC) (Hammond et al., 2000; Tomari and Zamore, 2005), of which Argonaute protein (AGO) is the slicer component showing similarity to RNase H (Liu et al., 2004; Song et al., 2004; Tomari and Zamore, 2005). Specific recognition of target sequences is guided by sRNAs through a base-pairing mechanism, whereas the slicing of target RNAs is carried out by the AGO proteins. Alternatively, the target RNA can be inactivated by translational arrest but this mechanism is still unclear (Brodersen et al., 2008; Hammond et al., 2001; Tomari and Zamore, 2005).

Plant viruses are strong inducers as well as targets of RNA silencing, and usually virus-derived small interfering RNAs (vsiRNAs) accumulate at high levels during viral infections. However, the origin of vsiRNAs is still far from being fully understood. The vsiRNAs are thought to be processed from viral dsRNA replicative intermediates, from local self-complementary regions of the viral genome (Molnar et al., 2005; Szittya et al., 2010) or from dsRNAs resulting from the action of RNA-dependent RNA polymerases (RDRs) on viral RNA templates (Garcia-Ruiz et al., 2010; Ruiz-Ferrer and Voinnet, 2009; Wang et al., 2010).

In plants two distinct classes of vsiRNA have been identified: the primary siRNAs, which result from DCL-mediated cleavage of an initial trigger RNA, and secondary siRNAs, whose biogenesis requires an RDR (Dunoyer et al., 2005; Wassenegger and Krczal, 2006). Recent reports suggest that dsRNAs synthesized by both viral and host RDRs are the predominant substrates for dicing (Wang et al., 2010), and secondary siRNAs derived from RDR6-mediated processed dsRNA drive a more effective antiviral response (Vaistij and Jones, 2009). However, this may not be a general rule and the outcome depends on the specific virus. We have shown recently that the vast majority of vsiRNAs accumulated in *Cymbidium ringspot virus*-infected plants are primary siRNAs and they efficiently activate the antiviral response in the lack-p19 silencing suppressor mutant (Szittya et al., 2010).

* Corresponding authors. V. Pantaleo and J. Burgyan are to be contacted at fax: +39 11 343809. P. Saldarelli, fax: +39 80 5443065.
E-mail addresses: v.pantaleo@ivv.cnr.it (V. Pantaleo), p.saldarelli@ba.ivv.cnr.it (P. Saldarelli), j.burgyan@ivv.cnr.its (J. Burgyan).
[1] These two authors equally contributed to the work.

0042-6822/$ – see front matter © 2010 Elsevier Inc. All rights reserved.
doi:10.1016/j.virol.2010.09.001

Most vsiRNAs are 21 or 22 nt in size and are the products of DCL4 and DCL2, which are the most important plant DICERs involved in virus-induced RNA silencing in *Arabidopsis thaliana* (Ruiz-Ferrer and Voinnet, 2009). Although DCL4 is the major player in vsiRNA production, in its absence DCL2 is also sufficient to produce 22 nt vsiRNAs, which are biologically active in antiviral silencing (Deleris et al., 2006; Fusaro et al., 2006). SiRNAs are associated with distinct Argonaute (AGO)-containing effector complexes to guide them to their RNA target molecules (Ding and Voinnet, 2007; Hutvagner and Simard, 2008; Vaucheret, 2008). In plants, loading of siRNAs into a particular AGO complex is preferentially, but not exclusively, dictated by their 5′ terminal nucleotides (Brodersen et al., 2008). AGO1 is the major slicer in plants but other AGO paralogs are likely to be involved, potentially also mediating translational repression (Brodersen et al., 2008; Ding and Voinnet, 2007).

Characterization of vsiRNAs by deep sequencing techniques, has mainly been done in experimental host plants whereas little is known about their genesis and processing in other species, except for recent reports on sweetpotato (Kreuze et al., 2009) and rice (Yan et al., 2010). On the other hand, in grapevine, Navarro et al. (2009) have given a thorough description of viroid-associated siRNAs (vdsiRNAs) and a couple of studies (Al Rwahnih et al., 2009; Coetzee et al., 2010) used deep sequencing for diagnostic purposes on purified total or double-stranded RNAs.

In this paper we characterize a subset of vsiRNAs detected in RNA samples from field-grown grapevine plants using a high-throughput approach to sequence total sRNAs from cv. Pinot Noir, clone ENTAV 115, whose genome has recently been sequenced (Velasco et al., 2007). We describe the features of vsiRNAs derived from several grapevine viruses infecting the same plant, in terms of size class abundance, polarities, and distribution along the viral genome.

Results and discussion

Composition of the vsiRNA population in grapevine

Libraries of total small RNAs from different grapevine tissues (leaves, berries, tendrils and flowers) were generated and sequenced, yielding ca. 3 to 6 million sequences *per* library. Molecules between 16 and 26 nt in size were selected. Detailed description of the libraries and processing of data are in Pantaleo et al. (2010).

The presence of a subset of 4559 vsiRNAs, comprehensive of all the four grapevine tissues explored was identified by BLASTN analysis searched against a database of viral genomic Reference Sequences (RefSeq) (Table 1) (Pruitt et al., 2007) with a tolerance limit of 0 mismatches. The analysis showed that the majority of reads were derived from grapevine-associated viruses such as *Grapevine Fleck virus* (GFkV, 3157 reads) and *Grapevine rupestris stem-pitting associated virus* (GRSPaV, 1106 reads). In addition, a small number of sequences were related to *Grapevine fanleaf virus* (GFLV, 29 reads). Surprisingly, small RNAs were identified from some members of the *Tymoviridae* which have never found associated with grapevine (i.e. *Turnip yellow mosaic virus*, TYMV (55 reads); *Ononis yellow mosaic virus*, OYMV (51 reads); *Oat blue dwarf virus*, OBDV (74 reads); *Okra mosaic virus*, OMV (43 reads); *Maize rayado fino virus*, MRFV (28 reads); and Citrus sudden death virus, CSDaV (16 reads). This is likely the consequence of the high degree of nucleotide homology within members of the *Tymoviridae* (Abou-Ghanem et al., 2003). Since the RefSeq database lacked all other tentative tymovirus species including Grapevine asteroid mosaic associated virus (GAMaV), Grapevine red globe virus (GRGV) and Grapevine rupestris vein feathering virus (GRVFV), we upgraded the database by adding all the GAMaV, GRGV and GRVFV sequences from the Entrez Nucleotide database (http://www.ncbi.nlm.nih.gov/sites/entrez?db=nuccore). Finally the new analysis (Table 1, Selected) allowed the identification of reads having homologies to these viruses which are respectively, in high number for GRGV (2138) and low for GAMaV (335) and GRVFV (190).

Table 1
Reads homologies identified by BLASTN analysis against a database containing viral genomic sequences (Refseq) and a database upgraded with viral sequences of the grapevine-infecting viruses (Selected) GRGV, GAMaV and GRVFV.

Virus species/genus	Database	
	Refseq	Selected
Grapevine fleck virus/*Maculavirus*	3157	3157
Grapevine rupestris stem-pitting associated virus/*Foveavirus*	1106	1106
Grapevine fanleaf virus/*Nepovirus*	29	29
Oat blue dwarf virus/*Marafivirus*	74	–
Turnip yellow mosaic virus/*Tymovirus*	55	–
Ononis yellow mosaic virus/*Tymovirus*	51	–
Okra mosaic virus/*Tymovirus*	43	–
Maize rayado fino virus/*Marafivirus*	28	–
Citrus sudden death-associated virus/*Marafivirus*	16	–
Grapevine red globe virus/*Maculavirus*	–	2138
Grapevine asteroid mosaic associated virus/*Marafivirus*	–	335
Grapevine rupestris vein feathering virus/*Marafivirus*	–	190
Total reads	4559	6955

Origin of vsiRNAs

The identification of vsiRNAs with homologies to specific viruses is evidence for the presence of these viruses in the plant examined. The presence of predicted virus species was further analyzed by RT-PCR using the primers listed in Table 2 (Fig. 1). The sequences of each amplicon plus additional sequences obtained, for some viruses, in different genomic regions, were deposited in the GenBank database under the accession numbers FN555301 and FN555302, (GRSPaV); FN555303, (GRGV); FN555304, (GFLV); FN555305, (GAMaV); FN555306, (GFKV). In the case of GRVFV, several sets of primers, even those designed on the vsiRNA sequences, did not succeed in detecting this virus. This may be due to its low titer in the tissue analyzed. Moreover, we did not find any evidence for the presence of Grapevine Syrah virus-1 (GSyV-1) using the primers described by Al Rwahnih et al. (2009).

The accumulation of vsiRNAs derived from the different viruses in the four grapevine tissues analyzed may suggest a limited tissue specificity. Indeed GFkV, GRGV and GAMaV (*Tymoviridae*) are phloem-restricted, GFLV replicates in primarily parenchyma cells and the specific localization of GRSPaV is unknown, although it occurs in both leaf tissues and cortical scrapings (Meng et al., 2005). Whereas GFkV vsiRNAs were mainly associated with flowers and tendrils, GRSPaV vsiRNAs were also quite abundant in small berries (Fig. 2). As a general trend for all the viruses, vsiRNAs were poorly represented in leaves compared to the other tissues (Fig. 2).

Size class analysis of vsiRNAs

The model plant *A. thaliana* encodes four Dicer-like proteins (DCLs), involved in both endogenous processes and antiviral RNA silencing (Ruiz-Ferrer and Voinnet, 2009). The homologs of the four *Arabidopsis* Dicers have been also been identified in the grapevine genome (Jaillon et al., 2007; Velasco et al., 2007). This prompted us to analyze the distribution of vsiRNAs in grapevine in order to find similarities and differences compared with model systems such as *Nicotiana benthamiana* and *A. thaliana*. For all the viruses, the prevalent vsiRNA size in the four tissues was 21 nt (4532 reads, corresponding to 65% of the total vsiRNAs) followed by 22 nt species (1044 reads, corresponding to 15% of the total vsiRNAs), together representing ca. 80% of the total (Fig. 2). The occurrence of 22 nt vsiRNAs was rated at 13%, 12%, 4% and 6%, for GRVFV, GRSPaV, GRGV and GAMaV respectively, whereas for GFkV it was at the relatively higher level of 24%. Distribution of vsiRNAs did not change in the individually analyzed libraries originating from flower, tendril, leaf and berry, indicating the absence of any tissue bias (Fig. 2). The

Table 2
Oligonucleotides used for cloning and detection of viral sequences (orientations toward viral genome is indicated).

Target	Name/orientation	Sequence	Reference
GRSPaV	GRSPaV E/sense	CGATAAACATAACAACAG	This study
GRSPaV	GRSPaV F/antisense	GAGAGCTGTAGCAGAAAC	This study
GRSPaV	GRSPaV G/sense	GAGATGCTCAATTTCAGGC	This study
GRSPaV	49r/antisense	GGGTGGGGATGTAGTAACTTTTGA	Zhang et al. (1998)
GRSPaV	GRSPaV H/antisense	CCTACAAACTCAAATGCTGAC	This study
GRSPaV	GRSPaV for/sense	GGGTGGGGATGTAGTAACTTTTGA	Gambino and Gribaudo (2006)
18S rRNA	Forward	CGCATCATTCAAATTTCTGC	Gambino and Gribaudo (2006)
18S rRNA	Reverse	TTCAGCCTTGCGACCATACT	Gambino and Gribaudo (2006)
GFLV	H2999/sense	TCGGGTGAGACTGCGCAACTTCCTA	Johnson R. *personal communication*
GFLV	C3310/antisense	GATGGTAACGCTCCCGCTGCTCTT	Johnson R. *personal communication*
GFkV	Fk-F/sense	CTCTCCGCCTCGTCTGATGAGC	Sabanadzovic S. *personal communication*
GFkV	Fk-R/antisense	GACTCGGTGCCCGTGATGTCATAC	Sabanadzovic S. *personal communication*
GRGV	RG-F/sense	TCGACACTCTCTCCATTTTCCGGG	Sabanadzovic S. *personal communication*
GRGV	RG-R/antisense	GTAGGAGGGGTTCTTTGGGAACACG	Sabanadzovic S. *personal communication*
GAMaV	AM-F/sense	CCCTTCTCCCTCTCAAAGGCGG	Sabanadzovic S. *personal communication*
GAMaV	AM-R/antisense	GGAGCTCCGCATGGCGGTAGTT	Sabanadzovic S. *personal communication*
GRVFV	VF-F/sense	CGAAGCTCACTGGCGGACTTCTG	Sabanadzovic S. *personal communication*
GRVFV	VF-R/antisense	GGCACAGAAGCCAAGGCGTTCA	Sabanadzovic S. *personal communication*
GSyV-1	GSyV-1Det-F/sense	CAAGCCATCCGTGCATCTGG	Al Rwahnih et al. (2009)
GsyV-1	GSyV-1Det-R/antisense	GCCGATTTGGAACCCGATGG	Al Rwahnih et al. (2009)
GFkV	GFKV A/sense	TCTCCAGCCTCAACCCCAC	This study
GFkV	GFkV B/antisense	AACCGAGGGCGACGCAGG	This study
GFkV	2421s/antisense	GGGATTGAAGCGGGGAAGAGG	This study
GFkV	5104s/sense	GTCCGCATCTTCTCGAAGACC	This study
GFkV	5112a/antisense	CTTGTGCTGGGTCTTCGAGAAG	This study
GRSPaV	GRSPaV 84/antisense	TTGCGAGCACCTCTTCAACAG	This study

predominance of 21 and 22 nt sizes suggests that in grapevine, as in other plants (Ruiz-Ferrer and Voinnet, 2009) DCL4 and DCL2 play the main role in the genesis of vsiRNAs.

This size distribution mirrored the pathway of RNA silencing toward RNA viruses observed in *A. thaliana*, which relies on hierarchical activity of DCL4, DCL2 and DCL3 (Bouche et al., 2006; Deleris et al., 2006; Diaz-Pendon et al., 2007; Fusaro et al., 2006; Qi et al., 2009), although the presence of 24 nt vsiRNAs, presumably produced by DCL3, was negligible for the viruses analyzed. A defect in DCL3-dependent siRNA biogenesis can be excluded since we have previously described a massive presence of 24 nt long viroid-derived and endogenous siRNAs (Navarro et al., 2009; Pantaleo et al., 2010). The ratio of unique vsiRNA sequences to the total number of vsiRNAs ranged from 59% (for GRVFV and GFKV) to 77% (for GRSPaV), clearly representing the bulk of small RNA species (not shown).

The polarity of vsiRNAs

Analysis of vsiRNA strand polarity showed different pictures for GRSPaV, GFLV and the grapevine members of the *Tymoviridae*. Unexpectedly, a clear prevalence for antisense strands (Fig. 3) was observed for GFkV, GRGV and GAMaV, accounting for 89%, 92% and 75% of the total reads, respectively. Conversely, 61% and 73% of GRSPaV and GFLV vsiRNAs had genomic-sense polarity. No preferential vsiRNA size class was associated with either sense or antisense polarity, indicating that the different DCL enzymes do not show strand preference and that the prevalence of vsiRNAs of sense (i.e. GRSPaV and GFLV) or antisense (i.e. GFkV, GRGV and GAMaV) polarity must be due to other virus-specific factors. The predominance of antisense vsiRNAs originating from GFkV (and other related viruses all belonging to the family *Tymoviridae*), is an unprecedent finding for all plant viruses analyzed so far by high- or low-throughput techniques (Donaire et al., 2008, 2009; Ho et al., 2006; Molnar et al., 2005; Qi et al., 2009; Wang et al., 2010). Notably, also in the low-throughput sequencing analysis carried out by Carra et al. (2009), the orientation of the three GFkV vsiRNAs was antisense. Conversely, viruses belonging to several taxonomical groups but different from the *Tymoviridae*, showed a higher frequency of sense-strand vsiRNAs or 1:1 ratio of both polarities, in accordance with the models that presume their origin from highly structured single-stranded regions of the genomic-sense viral RNAs or from dsRNA, respectively (Csorba et al., 2009; Wang et al., 2010).

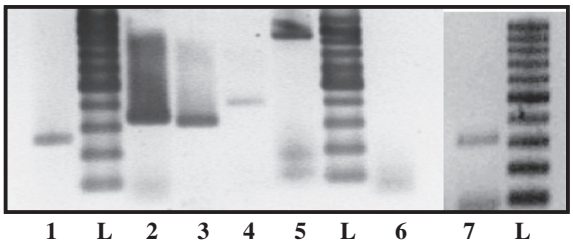

Fig. 1. Electrophoretic analysis of virus-specific PCR products amplified from total RNAs extracted from Pinot Noir ENTAV115 grapevine tissues. 1, GFkV (280 nt); 2, GRSPaV (340 nt); 3, GAMaV (320 nt); 4, GRGV (400 nt); 5, 18S rRNAs control (844 nt); 6, GSyV-1; 7, GFLV (312 nt); L, DNA ladder.

Our data suggest that the low abundance of antisense vsiRNAs compared to the sense vsiRNAs observed to date (Donaire et al., 2009; Ho et al., 2006; Molnar et al., 2005; Szittya et al., 2010) is not a general feature of all plant RNA viruses. Instead, the mechanisms responsible for strand polarity could depend on other factors related to a specific virus and not on the host, since in the same plant different viruses gave different vsiRNAs sense/antisense ratios. Attempts to estimate the ratio between the genomic/antigenomic GFkV viral RNAs in the grapevine tissues were unsuccessful (not shown). As for the genome features, a possible explanation might be found in the unusual composition of the *Tymoviridae* genome, which is rich in cytosines (Hellendoorn et al., 1996) and which account, in GFkV, GRGV, and GAMaV, respectively for 50%, 41% and 42% of the nucleotide content (Abou-Ghanem et al., 2003).

Distribution of first nucleotide vsiRNAs

VsiRNA reads of GFkV or GRSPaV were grouped by the first nucleotide (U, C, G, and A) and their relative abundance compared

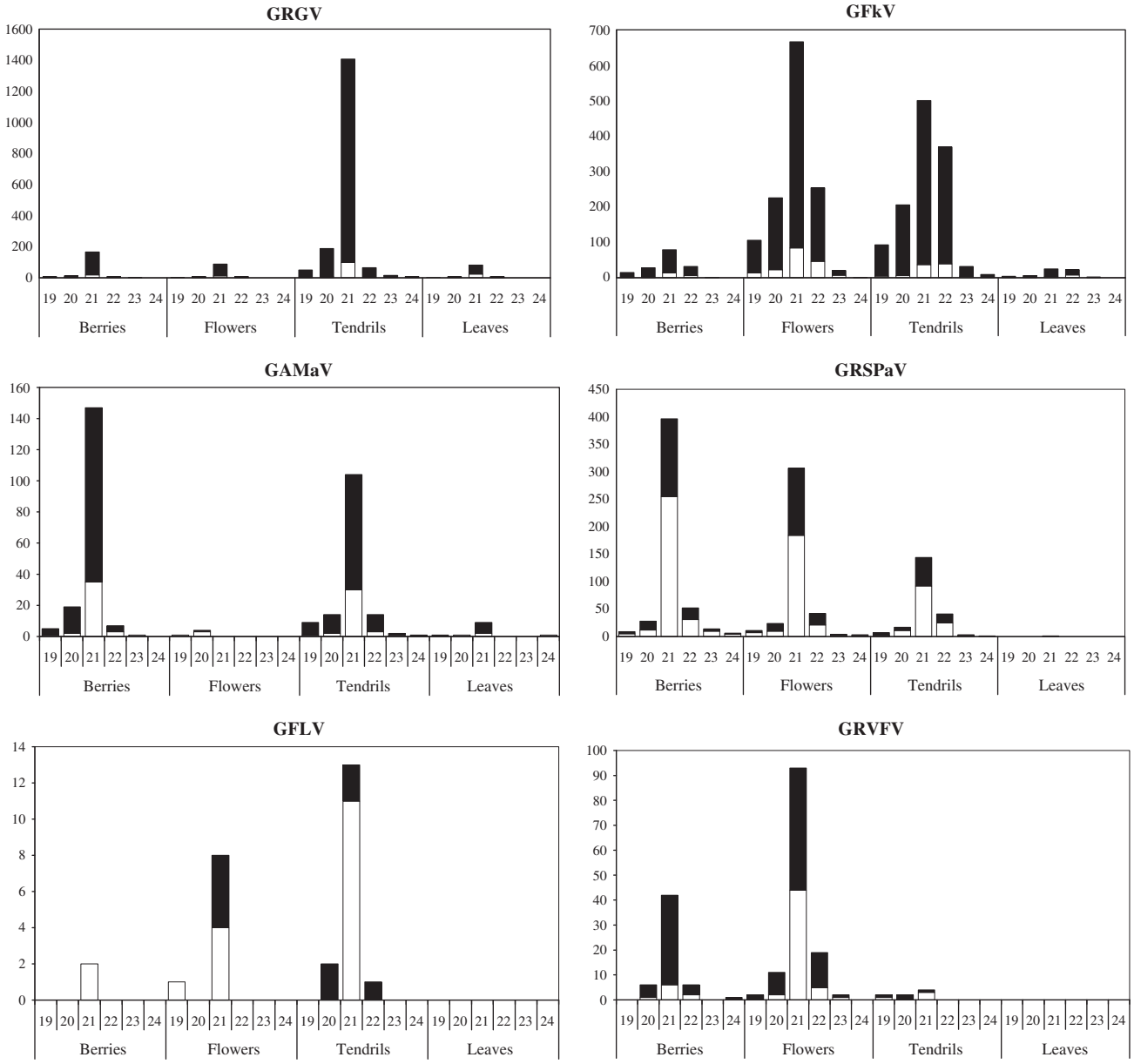

Fig. 2. Size distribution of total sequenced vsiRNAs for all the viruses. Numbers on the y axis refer to the reads obtained for each virus whereas, for the x axis, to the size of vsiRNAs. Sense and antisense polarities of vsiRNAs are indicated by open and filled bars, respectively.

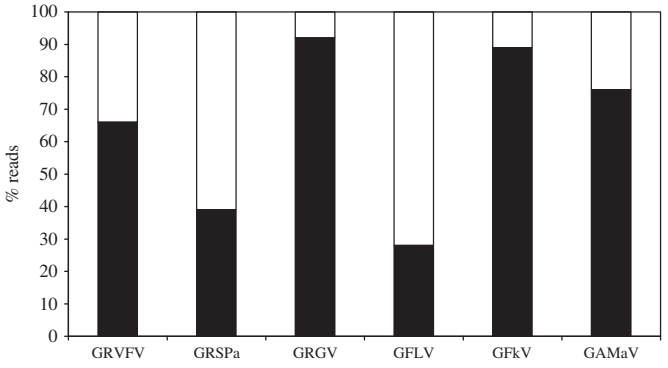

Fig. 3. Percentage distribution (y axis) of total sequenced vsiRNAs of all the viruses with respect to genome polarity. Sense and antisense polarities of vsiRNAs are indicated by open and filled bars, respectively.

with values expected from the nucleotide composition of sense and antisense strands. GRSPaV vsiRNAs showed a clear predominance of C at the 5′ end, whereas A and U were close to the expected values, considering both orientations and both unique and total sequence reads (Fig. 4A). This cytosine bias in the first position was even more evident considering that the nucleotide composition of GRSPaV genomic RNA is U(29%)>A(28%)>G(24%)>C(19%). These data clearly demonstrate an under-representation of Gs in the 5′ position.

Conversely, the 5′ terminal base for GFkV vsiRNAs (Fig. 4B) seems to be largely affected by their sense/antisense origin as well as by the features of the viral genome, which has 50% cytosine and guanine content in both the genomic and antigenomic strands (Hellendoorn et al., 1996). Accordingly, GFkV vsiRNA unique sequences of sense orientation show a preference for C at the 5′ end, whereas those of antisense orientation show a preference for G (Fig. 4B). The same, or even more accentuated, is observed for redundant GFkV vsiRNAs. GFkV vsiRNAs with sense polarity have a marked preference to have

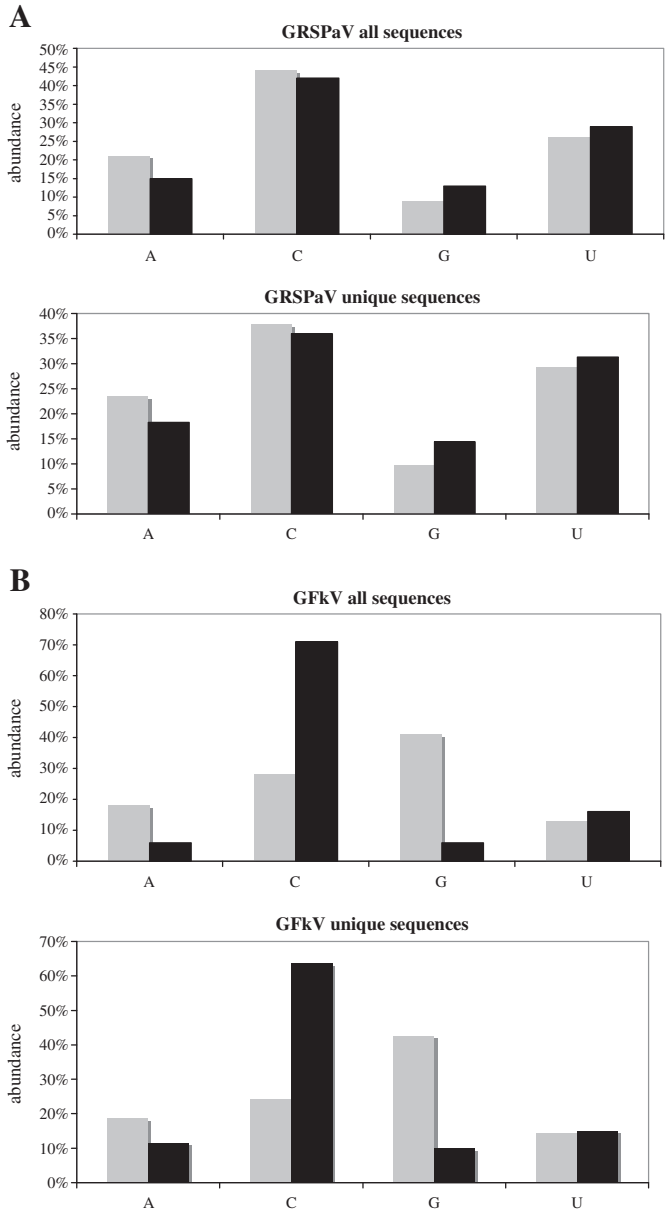

Fig. 4. 5′ terminal nucleotide abundance of GRSPaV (A) and GFkV (B) vsiRNA analyzed as unique or total sequences and distinguished as sense (gray bars) or antisense (filled bars) polarity with respect to the viral genome.

C > U > A and avoid G at 5′ end. This C preference of 64% (unique sequences) or 71% (redundant sequences), significantly exceeds the 50% C content of GFkV viral RNA, confirming the bias at the 5′ nucleotide position in vsiRNAs generated in grapevine. Similarly, 43% unique and 41% redundant vsiRNAs, deriving from the antigenomic GFkV RNA, started with G. The presence of G at the 5′ end is lower than expected from the genome composition (50% G) of the viral antigenomic strand. This finding again suggests a tendency to avoid G at the 5′ end of vsiRNAs.

Finally, no differences were found when investigating the 5′ terminal nucleotide preference within the 21-, 22- and 24-nucleotide size classes of vsiRNAs, suggesting that no bias was introduced by the different DCL enzymes.

Short RNAs could have differential stability in the cell based on the 5′ nucleotide-dependent sorting to associate with different AGO proteins (Mi et al., 2008). Indeed, a recent analysis of TuMV vsiRNAs has shown an overrepresentation of U at the 5′ end (Garcia-Ruiz et al., 2010) suggesting that a 5′ terminal U stabilizes vsiRNAs *in vivo* through association with AGO1, the main Argonaute protein involved in RNA silencing antiviral defence (Baumberger et al., 2007; Morel et al., 2002; Zhang et al., 2006).

Interestingly, both GFkV and GRSPaV display, at the 5′ terminal position of vsiRNAs, a C prevalence, and a clear tendency to reject a G (Fig. 4B). It has been shown that in *Arabidopsis* sRNAs or vsiRNAs with a C residue at the 5′ end are preferentially recruited by AGO5 (Mi et al., 2008; Takeda et al., 2008), whose function has not been explored. Furthermore, similar bias was observed for viroid-derived siRNAs in grapevine (Navarro et al., 2009). Whether or not vsiRNAs in such a natural system are mainly present in specific effector complexes and whether grapevine DCLs and AGOs have the same properties as the homologous proteins in *Arabidopsis* could be subjects for further study.

Mapping vsiRNAs along GRSPaV and GFkV genomic RNAs

The distribution of vsiRNAs was determined along the corresponding GRSPaV and GFkV genomes, since both viruses showed a high number of reads and full genome sequences are available. The GRSPaV genome was covered to 55% by unique vsiRNAs of all size classes and both sense orientations (Fig. 5A), the remaining unoccupied nucleotides being evenly distributed. Conversely, GFkV genome representation dropped to 45% with large regions not represented by small RNAs (Fig. 5B), particularly between nucleotides 2238 to 2671, 4772 to 4962 and 7162 to 7382. In these limited regions a high content of unpaired cytosines (guanines on the antisense strand) could hamper the formation of secondary structures potentially targeted by DCL enzymes, an idea supported by G/C skew values which were incompatible with foldback structures (G/C skew values: −0.62 for regions 2238–2671, −0.57 for regions 4772–4962 and −0.67 for regions 7162–7382).

Several vsiRNA-generating regions (hot spots) were identified, which in some cases were also confirmed *in vivo* by Northern blots (Fig. 6). In these hot spots, distinct vsiRNA species redundantly accumulated (indicated by G1 to G5 or R1 to R3 in Figs. 5A and B, respectively). In GRSPaV, hot spots were located in the extreme 5′ end around nucleotide 84 (R1) and in two positions in the last 1700 nucleotides (R2 and R3). A possible origin of R2 and R3 hotspots might be the generation and accumulation of 3′ co-terminal subgenomic RNAs during the virus life cycle.

GFkV also showed several hotspots (G1 to G5), all except G4 composed of antisense vsiRNAs. The distribution of hotspots did not correlate with the theoretical position of GFkV subgenomic RNAs. Analysis of vsiRNAs within the hotspots showed that both 21 and 22 nt vsiRNAs from both viruses accumulated at similar levels (not shown), suggesting an overlapping activity of DCL enzymes recognizing similar RNA molecules or structures. Confirmation of GFkV sequencing data was obtained by Northern blot analysis since no vsiRNA was detected in the 2238–2671 region (Fig. 6A) using an internal probe, whereas a signal was visible in position G4, corresponding to a hot spot generating either sense or antisense vsiRNAs (Fig. 6B). Attempts to identify *in vivo* vsiRNAs from GRSPaV hot spot R1, were unsuccessful. Therefore, the data suggest that GRSPaV and GFkV vsiRNAs preferentially originate from distinct positions, which are not evenly spread along the genome.

Conclusions

VsiRNAs analyzed in the present work were derived from grapevines grown in the field for several years, which likely explains their multiple infection status. Our study differs from previous analyses in which vsiRNAs originated from experimentally infected permissive hosts such as *N. benthamiana* and *A. thaliana*. It also highlights the high diversity of vsiRNAs depending on their specific virus origin. The use

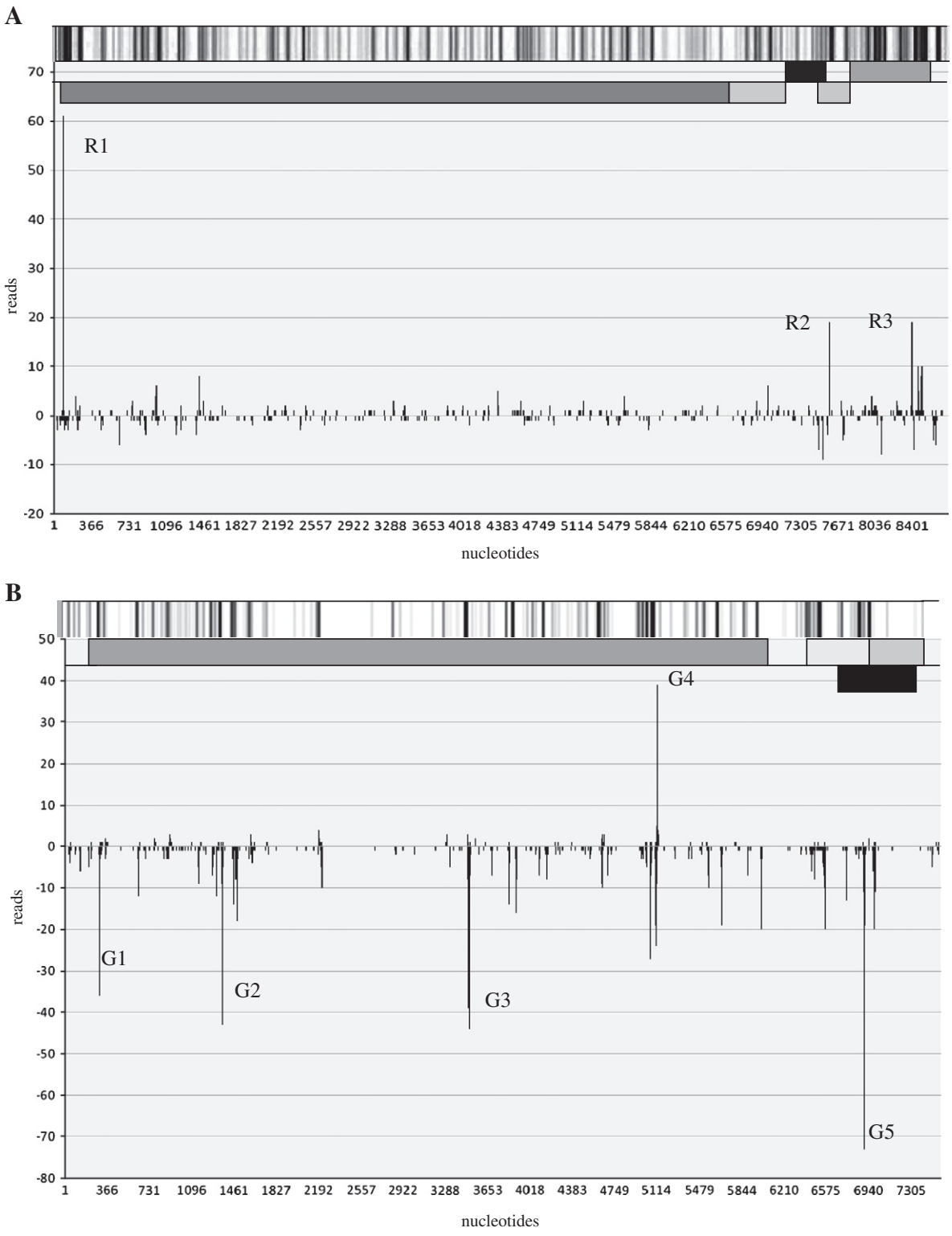

Fig. 5. Profile distribution of vsiRNAs of GRSPaV (A) and GFkV (B) with respect to their viral genomes. The bars above each schematic viral genome represent the genome coverage of unique vsiRNAs at each nucleotide position. More intense black bars are obtained by the overlapping or close association of different vsiRNAs whereas white regions correspond to nucleotides not covered by any vsiRNA. The graph displays vsiRNA total reads along the two genomes. Hot spot positions accumulating vsiRNAs in precise positions are indicated by R1–3 and G1–5. Peaks above and below the x axis stand respectively for sense and antisense vsiRNA orientations.

of deep sequencing of vsiRNAs in grapevine will be of great help in understanding plant pathogen interactions. The availability of two sequenced grapevine genomes (Jaillon et al., 2007; Velasco et al., 2007) allows study of antiviral RNA silencing pathways, currently explored only in herbaceous model plants, to be expanded to a woody plant system in field conditions.

Materials and methods

RNA isolation and RT-PCR detection

Total RNA was extracted from leaves or phloem tissues with the silica capture protocol (Rott and Jelkmann, 2001). Two-step RT-PCR

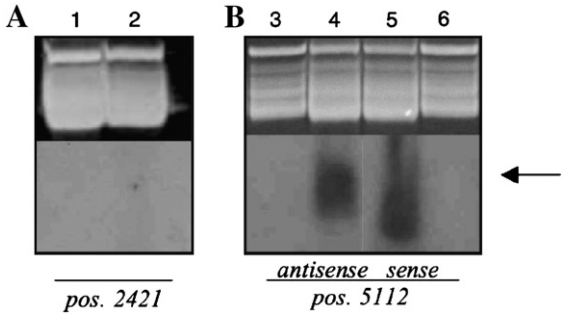

Fig. 6. Northern blot analysis of GFkV-related vsiRNAs. A) Gel blot analysis of siRNAs purified from healthy (1) and Pinot Noir ENTAV 115 grapevine tissues (2). The membrane was probed with the genome-sense probe 2421s. B) Gel blot analysis of siRNAs purified from healthy (3 and 6) and ENTAV 115 tissues (4 and 5). The membrane was probed with antisense (3 and 4) and sense (5 and 6) oligonucleotides 5112a and 5104s, respectively. Position of the 21 nt RNA marker is indicated.

was carried out as previously described (Saldarelli et al., 2006). PCR primers were from Al Rwahnih et al. (2009) and Abou-Ghanem et al. (2003) or designed in the present work, as in Table 2.

Cloning and sequencing of siRNAs

Total RNA was extracted from leaf, tendril, small berry (1–4 mm, in diameter) and inflorescence tissues of the Pinot Noir clone ENTAV 115, using guanidine thiocyanate buffer (Pantaleo et al., 2010). Low molecular weight RNA (LMWR) was further enriched by using the Qiagen RNA/DNA midi kit and following the manual's procedures. LMWR was used to generate libraries of short RNAs as previously described (Pantaleo et al., 2010). Deep sequencing was done on the Illumina Solexa platform using the standard manufacturer's protocol.

Analysis of vsiRNAs

The 5′ and 3′ adapter sequences were trimmed from the Solexa reads and vsiRNAs were identified by BLASTN software (Altschul et al., 1990) against the NCBI viral genomic sequences database (ftp://ftp.ncbi.nih.gov/refseq/release/viral/). VsiRNAs were aligned on reference genomes using SOAP software (Short Oligonucleotide Alignment Software; (Li et al., 2008) and the output file was visualized by Map View 3.4.1. (Bao et al., 2009). The G/C skew calculation was based on the formula (G) − (C) / (G) + (C). Plotting of vsiRNAs along the viral genome was accomplished by Excel analysis (version 11.5.5, Microsoft Corporation).

Acknowledgments

In memory of Dr. Robert G. Milne, with appreciation for his critical reading of and valuable comments to this paper. He passed suddenly away after the paper was accepted. This work was supported by the European Union funded FP6 Integrated Project SIROCCO (LSHG-CT-2006-037900) to J.B. Grapevine tissues were collected during a research visit funded by the bilateral research program CNR-MTA.

References

Abou-Ghanem, N., Sabanadzovic, S., Martelli, G.P., 2003. Sequence analysis of the 3′ end of three Grapevine fleck virus-like viruses from grapevine. Virus Genes 27, 11–16.
Al Rwahnih, M., Daubert, S., Golino, D., Rowhani, A., 2009. Deep sequencing analysis of RNAs from a grapevine showing Syrah decline symptoms reveals a multiple virus infection that includes a novel virus. Virology 387, 395–401.
Altschul, S.F., Gish, W., Miller, W., Myers, E.W., Lipman, D.J., 1990. Basic local alignment search tool. J. Mol. Biol. 215, 403–410.
Bao, H., Guo, H., Wang, J., Zhou, R., Lu, X., Shi, S., 2009. MapView: visualization of short reads alignment on a desktop computer. Bioinformatics 25, 1554–1555.
Bartel, D.P., 2004. MicroRNAs: genomics, biogenesis, mechanism, and function. Cell 116, 281–297.
Baulcombe, D., 2004. RNA silencing in plants. Nature 431, 356–363.
Baumberger, N., Tsai, C.H., Lie, M., Havecker, E., Baulcombe, D.C., 2007. The Polerovirus silencing suppressor P0 targets ARGONAUTE proteins for degradation. Curr. Biol. 17, 1609–1614.
Bernstein, E., Caudy, A.A., Hammond, S.M., Hannon, G.J., 2001. Role for a bidentate ribonuclease in the initiation step of RNA interference. Nature 409, 363–366.
Bouche, N., Lauressergues, D., Gasciolli, V., Vaucheret, H., 2006. An antagonistic function for *Arabidopsis* DCL2 in development and a new function for DCL4 in generating viral siRNAs. Embo J. 25, 3347–3356.
Brodersen, P., Sakvarelidze-Achard, L., Bruun-Rasmussen, M., Dunoyer, P., Yamamoto, Y.Y., Sieburth, L., Voinnet, O., 2008. Widespread translational inhibition by plant miRNAs and siRNAs. Science 320, 1185–1190.
Carra, A., Mica, E., Gambino, G., Pindo, M., Moser, C., Pè, M.E., Schubert, A., 2009. Cloning and characterization of small non-coding RNAs from grape. Plant J. 5, 750–763.
Coetzee, B., Freeborough, M.J., Maree, H.J., Celton, J.M., Rees, D.J., Burger, J.T., 2010. Deep sequencing analysis of viruses infecting grapevines: virome of a vineyard. Virology 400, 157–163.
Csorba, T., Pantaleo, V., Burgyan, J., 2009. RNA silencing: an antiviral mechanism. Adv. Virus Res. 75, 35–71.
Deleris, A., Gallego-Bartolome, J., Bao, J., Kasschau, K.D., Carrington, J.C., Voinnet, O., 2006. Hierarchical action and inhibition of plant Dicer-like proteins in antiviral defense. Science 313, 68–71.
Diaz-Pendon, J.A., Li, F., Li, W.X., Ding, S.W., 2007. Suppression of antiviral silencing by cucumber mosaic virus 2b protein in *Arabidopsis* is associated with drastically reduced accumulation of three classes of viral small interfering RNAs. Plant Cell 19, 2053–2063.
Ding, S.W., Voinnet, O., 2007. Antiviral immunity directed by small RNAs. Cell 130, 413–426.
Donaire, L., Barajas, D., Martinez-Garcia, B., Martinez-Priego, L., Pagan, I., Llave, C., 2008. Structural and genetic requirements for the biogenesis of tobacco rattle virus-derived small interfering RNAs. J. Virol. 82, 5167–5177.
Donaire, L., Wang, Y., Gonzalez-Ibeas, D., Mayer, K.F., Aranda, M.A., Llave, C., 2009. Deep-sequencing of plant viral small RNAs reveals effective and widespread targeting of viral genomes. Virology 392, 203–214.
Dunoyer, P., Himber, C., Voinnet, O., 2005. DICER-LIKE 4 is required for RNA interference and produces the 21-nucleotide small interfering RNA component of the plant cell-to-cell silencing signal. Nat. Genet. 37, 1356–1360.
Fusaro, A.F., Matthew, L., Smith, N.A., Curtin, S.J., Dedic-Hagan, J., Ellacott, G.A., Watson, J.M., Wang, M.B., Brosnan, C., Carroll, B.J., Waterhouse, P.M., 2006. RNA interference-inducing hairpin RNAs in plants act through the viral defence pathway. EMBO Rep. 7, 1168–1175.
Gambino, G., Gribaudo, I., 2006. Simultaneous detection of nine grapevine viruses by multiplex reverse transcription-polymerase chain reaction with coamplification of a plant RNA as internal control. Phytopathology 96, 1223–1229.
Garcia-Ruiz, H., Takeda, A., Chapman, E.J., Sullivan, C.M., Fahlgren, N., Brempelis, K.J., Carrington, J.C., 2010. *Arabidopsis* RNA-dependent RNA polymerases and Dicer-like proteins in antiviral defense and small interfering RNA biogenesis during Turnip mosaic virus infection. Plant Cell 22, 481–496.
Hamilton, A.J., Baulcombe, D.C., 1999. A species of small antisense RNA in posttranscriptional gene silencing in plants. Science 286, 950–952.
Hamilton, A., Voinnet, O., Chappell, L., Baulcombe, D., 2002. Two classes of short interfering RNA in RNA silencing. Embo J. 21, 4671–4679.
Hammond, S.M., Bernstein, E., Beach, D., Hannon, G.J., 2000. An RNA-directed nuclease mediates post-transcriptional gene silencing in *Drosophila* cells. Nature 404, 293–296.
Hammond, S.M., Boettcher, S., Caudy, A.A., Kobayashi, R., Hannon, G.J., 2001. Argonaute2, a link between genetic and biochemical analyses of RNAi. Science 293, 1146–1150.
Hellendoorn, K., Mat, A.W., Gultyaev, A.P., Pleij, C.W., 1996. Secondary structure model of the coat protein gene of turnip yellow mosaic virus RNA: long, C-rich, single-stranded regions. Virology 224, 43–54.
Ho, T., Pallett, D., Rusholme, R., Dalmay, T., Wang, H., 2006. A simplified method for cloning of short interfering RNAs from *Brassica juncea* infected with Turnip mosaic potyvirus and Turnip crinkle carmovirus. J. Virol. Meth. 136, 217–223.
Hutvagner, G., Simard, M.J., 2008. Argonaute proteins: key players in RNA silencing. Nat. Rev. Mol. Cell Biol. 9, 22–32.
Jaillon, O., Aury, J.M., Noel, B., Policriti, A., Clepet, C., Casagrande, A., Choisne, N., Aubourg, S., Vitulo, N., Jubin, C., Vezzi, A., Legeai, F., Hugueney, P., Dasilva, C., Horner, D., Mica, E., Jublot, D., Poulain, J., Bruyere, C., Billault, A., Segurens, B., Gouyvenoux, M., Ugarte, E., Cattonaro, F., Anthouard, V., Vico, V., Del Fabbro, C., Alaux, M., Di Gaspero, G., Dumas, V., Felice, N., Paillard, S., Juman, I., Moroldo, M., Scalabrin, S., Canaguier, A., Le Clainche, I., Malacrida, G., Durand, E., Pesole, G., Laucou, V., Chatelet, P., Merdinoglu, D., Delledonne, M., Pezzotti, M., Lecharny, A., Scarpelli, C., Artiguenave, F., Pe, M.E., Valle, G., Morgante, M., Caboche, M., Adam-Blondon, A.F., Weissenbach, J., Quetier, F., Wincker, P., 2007. The grapevine genome sequence suggests ancestral hexaploidization in major angiosperm phyla. Nature 449, 463–467.
Kim, V.N., 2005. Small RNAs: classification, biogenesis, and function. Mol. Cells 19, 1–15.
Kreuze, J.F., Perez, A., Untiveros, M., Quispe, D., Fuentes, S., Barker, I., Simon, R., 2009. Complete viral genome sequence and discovery of novel viruses by deep sequencing of small RNAs: a generic method for diagnosis, discovery and sequencing of viruses. Virology 388, 1–7.
Li, R., Li, Y., Kristiansen, K., Wang, J., 2008. SOAP: short oligonucleotide alignment program. Bioinformatics 24, 713–714.
Liu, J., Carmell, M.A., Rivas, F.V., Marsden, C.G., Thomson, J.M., Song, J.J., Hammond, S.M., Joshua-Tor, L., Hannon, G.J., 2004. Argonaute2 is the catalytic engine of mammalian RNAi. Science 305, 1437–1441.

Meng, B., Li, C., Wang, W., Goszczynski, D., Gonsalves, D., 2005. Complete genome sequences of two new variants of Grapevine rupestris stem pitting-associated virus and comparative analyses. J. Gen. Virol. 86, 1555–1560.

Mi, S., Cai, T., Hu, Y., Chen, Y., Hodges, E., Ni, F., Wu, L., Li, S., Zhou, H., Long, C., Chen, S., Hannon, G.J., Qi, Y., 2008. Sorting of small RNAs into *Arabidopsis* argonaute complexes is directed by the 5′ terminal nucleotide. Cell 133, 116–127.

Molnar, A., Csorba, T., Lakatos, L., Varallyay, E., Lacomme, C., Burgyan, J., 2005. Plant virus-derived small interfering RNAs originate predominantly from highly structured single-stranded viral RNAs. J. Virol. 79, 7812–7818.

Morel, J.B., Godon, C., Mourrain, P., Beclin, C., Boutet, S., Feuerbach, F., Proux, F., Vaucheret, H., 2002. Fertile hypomorphic ARGONAUTE (ago1) mutants impaired in post-transcriptional gene silencing and virus resistance. Plant Cell 14, 629–639.

Navarro, B., Pantaleo, V., Gisel, A., Moxon, S., Dalmay, T., Bisztray, G., Di Serio, F., Burgyan, J., 2009. Deep sequencing of viroid-derived small RNAs from grapevine provides new insights on the role of RNA silencing in plant–viroid interaction. PLoS ONE 4, e7686.

Pantaleo, V., Moxon, S., Miozzi, L., Moulton, V., Dalmay, T., Burgyan, J., 2010. Identification of grapevine microRNAs and their targets using high throughput sequencing and degradome analysis. Plant J. 62, 960–976.

Plasterk, R.H., 2002. RNA silencing: the genome's immune system. Science 296, 1263–1265.

Pruitt, K.D., Tatusova, T., Maglott, D.R., 2007. NCBI reference sequences (RefSeq): a curated non-redundant sequence database of genomes, transcripts and proteins. Nucleic Acids Res. 35, D61–D65 (Database issue).

Qi, X., Bao, F.S., Xie, Z., 2009. Small RNA deep sequencing reveals role for *Arabidopsis thaliana* RNA-dependent RNA polymerases in viral siRNA biogenesis. PLoS ONE 4, e4971.

Rott, M.E., Jelkmann, W., 2001. Detection and partial characterization of a second closterovirus associated with Little cherry disease, Little cherry virus-2. Phytopathology 91, 261–267.

Ruiz-Ferrer, V., Voinnet, O., 2009. Roles of plant small RNAs in biotic stress responses. Ann. Rev. Plant Biol. 60, 485–510.

Saldarelli, P., Vigne, E., Talas, F., Bronnenkant, I., Dridi, A.M., Andret-Link, P., Boscia, D., Gugerli, P., Fuchs, M., Martelli, G.P., 2006. Partial characterization of two divergent variants of Grapevine leafroll-associated virus 4. J. Plant Pathol. 88, 203–214.

Song, J.J., Smith, S.K., Hannon, G.J., Joshua-Tor, L., 2004. Crystal structure of Argonaute and its implications for RISC slicer activity. Science 305, 1434–1437.

Szittya, G., Moxon, S., Pantaleo, V., Toth, G., Rusholme-Pilcher, R.L., Moulton, V., Burgyan, J., Dalmay, T., 2010. Structural and functional analysis of viral siRNAs. PLoS Pathog. 6 (4), e1000838.

Takeda, A., Iwasaki, S., Watanabe, T., Utsumi, M., Watanabe, Y., 2008. The mechanism selecting the guide strand from small RNA duplexes is different among argonaute proteins. Plant Cell Physiol. 49, 493–500.

Tomari, Y., Zamore, P.D., 2005. Perspective: machines for RNAi. Genes Dev. 19, 517–529.

Vaistij, F.E., Jones, L., 2009. Compromised virus-induced gene silencing in RDR6-deficient plants. Plant Physiol. 149, 1399–1407.

Vaucheret, H., 2008. Plant ARGONAUTES. Trends Plant Sci. 13, 350–358.

Velasco, R., Zharkikh, A., Troggio, M., Cartwright, D.A., Cestaro, A., Pruss, D., Pindo, M., Fitzgerald, L.M., Vezzulli, S., Reid, J., Malacarne, G., Iliev, D., Coppola, G., Wardell, B., Micheletti, D., Macalma, T., Facci, M., Mitchell, J.T., Perazzolli, M., Eldredge, G., Gatto, P., Oyzerski, R., Moretto, M., Gutin, N., Stefanini, M., Chen, Y., Segala, C., Davenport, C., Dematte, L., Mraz, A., Battilana, J., Stormo, K., Costa, F., Tao, Q., Si-Ammour, A., Harkins, T., Lackey, A., Perbost, C., Taillon, B., Stella, A., Solovyev, V., Fawcett, J.A., Sterck, L., Vandepoele, K., Grando, S.M., Toppo, S., Moser, C., Lanchbury, J., Bogden, R., Skolnick, M., Sgaramella, V., Bhatnagar, S.K., Fontana, P., Gutin, A., Van de Peer, Y., Salamini, F., Viola, R., 2007. A high quality draft consensus sequence of the genome of a heterozygous grapevine variety. PLoS ONE 2, e1326.

Wang, X.B., Wu, Q., Ito, T., Cillo, F., Li, W.X., Chen, X., Yu, J.L., Ding, S.W., 2010. RNAi-mediated viral immunity requires amplification of virus-derived siRNAs in *Arabidopsis thaliana*. Proc. Nat. Acad. Sci. U.S.A. 107, 484–489.

Wassenegger, M., Krczal, G., 2006. Nomenclature and functions of RNA-directed RNA polymerases. Trends Plant Sci. 11, 142–151.

Yan, F., Zhang, H., Adams, M.J., Yang, J., Peng, J., Antoniw, J.F., Zhou, Y., Chen, J., 2010. Characterization of siRNAs derived from rice stripe virus in infected rice plants by deep sequencing. Arch. Virol. 155, 935–940.

Zhang, X., Yuan, Y.R., Pei, Y., Lin, S.S., Tuschl, T., Patel, D.J., Chua, N.H., 2006. Cucumber mosaic virus-encoded 2b suppressor inhibits *Arabidopsis* Argonaute1 cleavage activity to counter plant defense. Genes Dev. 20, 3255–3268.

Zhang, Y.P., Uyemoto, J.K., Golino, D., Rowhani, A., 1998. Nucleotide sequence and RT-PCR detection of a virus associated with grapevine rupestris stem pitting disease. Phytopathology 88, 1231–1237.